

Spectral characterization of mechanically synthesized MoO₃-CuO nanocomposite

Dola Sundeep¹  · A. Gopala Krishna¹ · R. V. S. S. N. Ravikumar² · T. Vijaya Kumar⁴ · S. Daniel Ephraim³ · Y. L. Pavan⁴

Received: 3 September 2015 / Accepted: 19 December 2015 / Published online: 26 January 2016
© The Author(s) 2016. This article is published with open access at Springerlink.com

Abstract In this work, MoO₃-CuO metal oxide composite nanopowders are prepared by simple mechanochemical assisted synthesis technique with the stoichiometric weight ratios of MoO₃ and CuO as 2.3:1 and 3.3:1, respectively. The structural and spectroscopic properties of the as-synthesised samples are characterised by XRD, SEM with EDS, FT-IR, Raman spectroscopy and TGA/DTA. X-ray diffraction pattern demonstrates the peaks correspond to orthorhombic phase of α -MoO₃ and monoclinic phase of β -CuO. The average crystalline sizes of the 2.3:1 and 3.3:1 samples were found to be 16 and 24 nm, respectively, which are supported by Williamson–Hall (W–H) calculations. The correlations between the milling rotational speeds with morphological characteristics are revealed by the SEM images. The fundamental modes of Mo=O and Cu–O were analysed by FT-IR. Raman analysis has provided the qualitative information about the structure of the mixed oxide composite. Thermogravimetry analysis and

Differential Thermal Analysis (DTA) of MoO₃-CuO have revealed that the dual phase mixed oxide composite is stable up to 709 °C with a negligible weight loss. Based on the above, it can be inferred that the synthesised mixed lubricious oxide nanocomposite could be used as a solid lubricant at elevated temperatures.

Keywords Mixed oxide nanocomposites · Mechanochemical synthesis · Williamson–Hall plot · TGA and DTA

Introduction

Transition metal oxides have been attracted extensive attention due to their unique thermoelectric properties provided by the high temperature stability and tunable electronic and photon transport properties [1]. In addition, they have emerged as a promising area of research and attracted wide attention in the field of the nanotechnology for their vast applications as catalysts [2], sensors, and photochromatic devices [3, 4]. Metal oxides are extensively used for tribological applications [5–7]. Nanotechnology provides a vast area of research and assures excellent tribological properties [8]. Among these materials Molybdenum tri Oxide (MoO₃), n-type semiconductor with a wide band gap (>2.7 eV) is attractive due to its structural and optical properties [9, 10]. Molybdenum (VI) oxide (MoO₃) has distinctive electrochromic, thermochromic and photochromic properties, widely used as catalysts [11], sensors [12, 13] and lubricants [14]. In general, molybdenum (IV) oxide exists in three different phase structures as thermodynamically stable normal orthorhombic (α -MoO₃) [15, 16], monoclinic (β -MoO₃) and hexagonal (h-MoO₃)

✉ Dola Sundeep
sundeepdola@gmail.com; dolasundeep@gmail.com

A. Gopala Krishna
dr.a.gopalakrishna@gmail.com

¹ School of Nanotechnology, Institute of Science and Technology (IST), Jawaharlal Nehru Technological University (JNTUK), Kakinada 533003, Andhra Pradesh, India

² Department of Physics, Acharya Nagarjuna University, Nagarjuna Nagar, Guntur 522510, Andhra Pradesh, India

³ Department of Mechanical Engineering, Jawaharlal Nehru Technological University, Kakinada 533003, Andhra Pradesh, India

⁴ Department of Mechanical Engineering, K L University, Green Fields, Vaddeswaram, Guntur 522502, Andhra Pradesh, India

[17, 18]. Cupric oxide (CuO) is a p-type semiconductor with an indirect band gap of 1.2–1.5 eV [19]. CuO nanoparticles can also be used as solid lubricants due to their appreciable friction reduction properties [20, 21].

For lubrication applications, most of lamellar/layered solid lubricants fail in open air and high temperatures above 500 °C, as they turn into oxides [22]. Significant research has been carried out to use transition metal oxides as lubricants and to form alloys or composite structures for high capable lubricants at greater temperatures [23]. MoO₃ can be used as lubricant at high temperatures as it becomes soft and highly shareable at elevated temperatures [24]. For wider operational ranges these oxides can form into mixed oxides, i.e. alloys or composites for significant applications over mono oxide lubricants. Mixed Oxide such as MoO₃-CuO alloy or composite can provide enhanced frictional performance at different high temperatures [25, 26].

High energy ball milling is the most effective and simple synthesis technique used for large scale production of nanomaterials. Different forms of Nano structures such as metal–metal, metal–metalloid and metal–carbon can be produced using mechanical synthesis [27]. During ball milling the metallothermic reduction resulted composite powders are achieved due to the thermal energy generated during reactive milling [27]. Various techniques have been also used to produce the mixed oxide nanocomposites such as sol–gel [28], hydrothermal [29], Pulsed laser deposition [30] and mechanochemical synthesis [31, 32].

In the present investigation, MoO₃-CuO metal oxide composite nanopowders were prepared by mechanical activation assisted synthesis. The structural properties are found through spectroscopic characterizations such as X-ray diffraction (XRD), scanning electron microscope (SEM), Energy dispersive X-ray analysis (EDX), Fourier Transform Infrared (FT-IR) spectroscopy, Raman Spectroscopy, Thermogravimetric analysis (TGA) and Differential Thermal Analysis (DTA).

Experimental procedure

Materials

Molybdenum tri oxide (MoO₃) and Cupric Oxide (CuO) were purchased from Merck chemicals, India. The chemical reagents are of analytical grade and are used without any further purification. The chemicals used in the synthesis are of above 99 % purity.

Synthesis procedure

MoO₃ and CuO powders with mean particle size of 5 μm were considered in two samples. The samples were

prepared with different stoichiometric weight ratios of MoO₃ to CuO as 2.3:1 and 3.3:1 and were homogeneously mixed separately. These two sample mixtures were mechanically activated using high energy planetary ball mill (Retsch) with 50 ml vial and balls of zirconia as medium in milling, individually. Mechanical activation was performed using powder to ball ratio of 1:10. The milling was performed for 6 h with an interval pause of 5 min after every 30 min and with a rotational speed of 350 rpm, respectively. The obtained mixtures were taken in a crucible and calcinated in air for 40 h, after every 6 h the products were grounded and recalculated [31, 32]. Thus, MoO₃-CuO metal oxide nanocomposite powders were synthesised into 2.3:1 and 3.3:1 ratio sample powders and were named as sample A and B.

Characterisation

Powder X-ray diffraction (XRD) patterns of samples A and B were performed on a PANalytical XPert Pro-diffractometer with CuKα radiation ($\lambda = 1.5406 \text{ \AA}$), respectively. The measurements were made at room temperature at a range of 0°–70° on 2θ with a step size of 0.05°. Scanning Electron Microscope (SEM) images were obtained from a Carl Zeiss SEM EVO with carbon coating and Energy Dispersive X-ray Spectroscopy (EDS) images were taken from ZEISS EVO 18. Fourier Transform Infrared (FT-IR) spectrum was recorded using the KBr pellets on Shimadzu IRAffinity-1 FT-IR spectrophotometer in the region 4000–400 cm⁻¹. Raman measurements were obtained using mini Raman Microprobe Imaging system 3000 coupled to an optical microscope with spatial resolution of 1.5 μm and spectral resolution 2 cm⁻¹. Thermogravimetry analyses (TGA) and Differential thermal analysis (DTA) were carried out at a ramp rate of 10 °C min⁻¹, in nitrogen flow of 20 cm³ min⁻¹ using TGA/DTA-TA Instruments SDT Q600.

Results and discussion

Powder X-ray diffraction analyses studies

The crystal structural phases of synthesised sample powders were performed by the X-ray diffraction pattern. The XRD patterns of synthesised samples with two different compositions are shown in Fig. 1. The diffraction peaks of the composite exhibit two different phase structures coexisting [33] such as orthorhombic crystal system (α -MoO₃) with corresponding lattice cell parameters $a = 3.962$, $b = 13.858$, $c = 3.697$ nm and CuO exhibits monoclinic system with lattice parameters as $a = 4.692$, $b = 3.428$ and $c = 5.137$ nm. The diffraction peaks of chosen

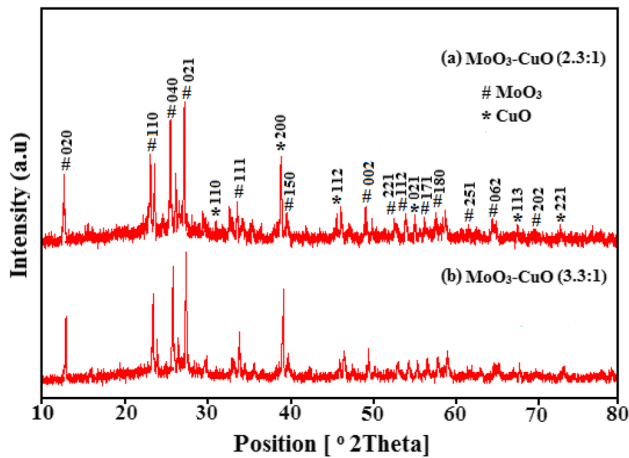


Fig. 1 X-ray diffraction patterns of **a** 2.3:1 and **b** 3.3:1 MoO₃-CuO metal oxide nanocomposite powders

samples along with their associated planes are listed in Table 1. All the diffraction peaks of the composite are well matched with the standard diffraction data of JCPDS file Nos. 05-0508 and 80-1916 for MoO₃ and CuO, respectively.

The existence of sharp diffraction peaks at 2θ located at 23.32°, 25.70°, 27.33° and 38.89° corresponding to (110), (040), (021) and (200) planes indicated the formation of a pure MoO₃-CuO composite nanoparticles. The estimation of crystalline size and lattice strain is done by simple and

powerful X-ray profile analysis [34]. The average crystalline sizes of the prepared samples were calculated using the Debye–Scherrer’s formula [35] as given in Eq. (1).

$$D = \frac{0.9 \lambda}{\beta \cos \theta} \text{ nm} \tag{1}$$

Where *D* is the crystalline size; λ is the wavelength of X-ray ($\lambda = 0.154056$ nm for (CuK α)); β is the Full Width at Half Maximum (FWHM) of the Bragg’s peak (in radians); θ is the diffraction angle of the reflection. The average crystalline size *D* is calculated from the diffraction peaks. It was found to be 16 and 25 nm for the sample A and the sample B, respectively. This shows that the crystalline size increases with increase in the MoO₃ content. A small shift in the position of the diffraction peaks towards higher angles is noted in sample A and broadening of XRD peak is seen due to the increase of ionic radius as CuO doped [36]. This shifting and broadening is negligible in sample B as the MoO₃ content is increased. The peak broadening in the XRD pattern indicates the presence of small nanocrystals in the samples. There is no evidence of any impurity or bulk material remnant. The shifting in the peak position and line broadening of the XRD pattern reveals the presence of micro strains in the sample. Micro strain is a measurement of distribution of lattice constants arising from crystal imperfection such as lattice dislocation. The micro strains (ϵ) induced broadening in powders due to crystal imperfection and distortion was calculated using Eq. (2) [37, 38].

Table 1 Diffraction peaks of 2θ and associated planes of 2.3:1 and 3.3:1 MoO₃-CuO metal oxide nanocomposites powders

S. no.	Standard 2θ	2.3:1 2θ	3.3:1 2θ	Planes h k l	Metal oxide
1	12.763	12.872	12.886	0 2 0	MoO ₃
2	23.327	23.449	23.432	1 1 0	MoO ₃
3	25.703	25.801	25.807	0 4 0	MoO ₃
4	27.333	27.425	27.431	0 2 1	MoO ₃
5	32.476	32.956	32.974	1 1 0	CuO
6	33.729	33.364	33.847	1 1 1	MoO ₃
7	38.891	38.250	38.643	2 0 0	CuO
8	39.652	39.063	39.063	1 5 0	MoO ₃
9	46.193	46.412	46.392	1 1 2	CuO
10	49.237	49.338	49.343	0 0 2	MoO ₃
11	54.125	54.133	54.147	2 2 1	MoO ₃
12	55.184	55.276	55.437	1 1 2	MoO ₃
13	56.642	56.433	56.439	0 2 1	CuO
14	57.673	57.798	57.747	1 7 1	MoO ₃
15	58.071	58.902	58.904	1 8 0	MoO ₃
16	62.865	62.876	62.972	2 5 1	MoO ₃
17	64.523	64.570	64.599	0 6 2	MoO ₃
18	67.848	67.640	67.621	1 1 3	CuO
19	69.460	69.690	69.686	2 0 2	MoO ₃
20	72.864	72.944	72.940	2 2 1	CuO

Bold values indicate the diffraction peaks and lattice parameters of CuO

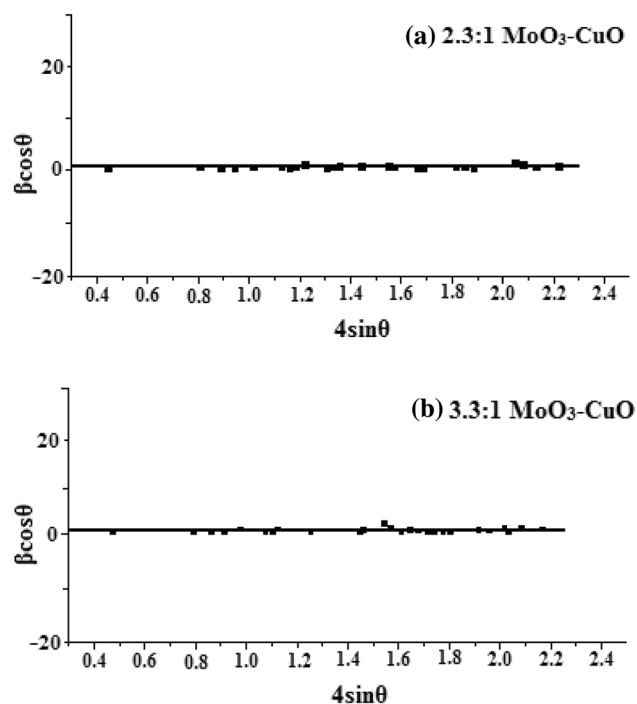


Fig. 2 W–H plot of **a** 2.3:1 and **b** 3.3:1 MoO₃-CuO metal oxide nanocomposite powders

$$\varepsilon = \frac{\beta \cos \theta}{4} \quad (2)$$

The high rotation of ball and the vial produce a twist in the crystal which results in screw like dislocations from ball milling. The grinding balls are accelerated through coriolis and centrifugal forces. A powerful impact forces are resulted between the balls and the sample materials as the material is powerfully accelerated from one side to other in the vial. X-ray line broadening was used to estimate the dislocation densities in the samples. The dislocation density (δ) was calculated by Eq. (3).

$$(\delta = 1/D^2) \quad (3)$$

Where D is the crystallite size.

Williamson–Hall analysis is a simplified integral breadth method employed for estimating crystal, crystallite size and lattice strain, considering the peak width as a function of 2θ [39]. The crystallite size is not necessary the same as particle size, since the crystallite size is assumed to

be the size of a coherently diffracting domain. From Eqs. (1) and (2), it is clear that the peak width from crystalline size varies as per the equation $\frac{1}{\cos\theta}$ and strain takes the equation $\tan\theta$. Assuming the particle size and the strain contributions to line broadening are independent to each other and both have Cauchy-like profile; the observed line breadth is taken as the sum of Eqs. (1) and (2),

$$\beta = \frac{0.9\lambda}{D\cos\theta} + 4\varepsilon \tan\theta \quad (4)$$

By rearranging Eq. (4), we get

$$\beta \cos\theta = \frac{0.9\lambda}{D} + 4\varepsilon \sin\theta \quad (5)$$

Equation (5) is Williamson–Hall equation [40], assumes the strain is uniform in all crystallographic directions. W–H equation represents a straight line between the $4\sin\theta$ (X-axis) and $\beta\cos\theta$ (Y-axis). The crystallite size (D) and micro strain (ε) are calculated from the intercept ($k\lambda/D$) and slope of the line. Figure 2 shows the (W–H) plots of the samples A and B. Micro strain of low molybdenum sample, i.e. A is greater than the B. Table 2 shows the average crystalline size, lattice strain and dislocation density of the nanocomposite samples. The crystalline sizes from debye–scherrer’s and micro strains calculated are compared with the calculations of W–H plots, and are found to be closely matched (Table 2).

Morphological studies

The morphological studies of samples are observed from SEM images. SEM analysis is an important for characterisation technique for topographic study of the samples and gives the information regarding the growth mechanism, shape and size of the particles. Figures 3 and 4 show the images of the samples A and B taken at different magnifications. The prepared samples contain rod and spherical like mixed structures, with irregular shape and dimensions. As the grain size from SEM images is the domains formed by the agglomeration of nanocrystalline [41], the grain sizes from the SEM images and the crystalline size calculated from the debye–scherrer’s and Williamson–Hall methods do not match as the grains seen in the SEM are the domains formed by aggregation of crystallites [41]. The

Table 2 Average crystallite size, micro strain and dislocation densities of 2.3:1 and 3.3:1 MoO₃-CuO mixed metal oxide nanocomposite powders

Sample MoO ₃ -CuO	Crystalline size (nm)		Micro strain ($\varepsilon \times 10^{-3}$)		Dislocation density ($\delta \times 10^{-15} \text{m}^{-2}$)
	Scherrer’s	W–H method	Calculated	W–H method	
2.3:1	16	17	0.02	0.48	1.73
3.3:1	25	26	0.013	0.038	3.90



EDS spectra are shown in Fig. 5. The presence of two metal oxides is confirmed from the EDS spectra. It is found that EDS data demonstrate that prepared samples are composed of Molybdenum (Mo), Oxygen (O) and Copper (Cu) species. As molybdenum was taken in more ratios, the EDS data resulted in the highest percentage of Molybdenum.

Table 3 Assignments of FT-IR vibration bands of 2.3:1 and 3.3:1 MoO₃-CuO metal oxide nanocomposite

2.3:1	3.3:1	Band assignment
496, 603	497, 603	Cu–O
992	992	Mo=O
873	870	Mo–O–Mo
1384, 1643	1384, 1643	Mo–OH

FT-IR studies

FT-IR spectra of the samples are shown in Fig. 6, which are acquired in the range of 4000–400 cm⁻¹. When a molecule interacts with light, it corresponds to the change in the dipole moment of a molecule resulting in the Infrared IR band. The characteristic bands observed at 497, 603 and 992 cm⁻¹ are attributed to the fundamental vibrational modes of Cu–O [42] and Mo=O [43]. The successive synthesis of MoO₃-CuO metal oxide nanocomposite is shown by the characteristic bands. Generally MoO₃ exhibits 17 IR active modes. The formation of as-synthesised nanocomposite is also confirmed by the X-ray diffraction (XRD) and EDS spectra. The dominion band at 870 cm⁻¹ is associated with the vibration of Mo–O–Mo bridging bonds [44]. The absorption bands detected at 1387 and 1643 cm⁻¹ are associated with the vibration

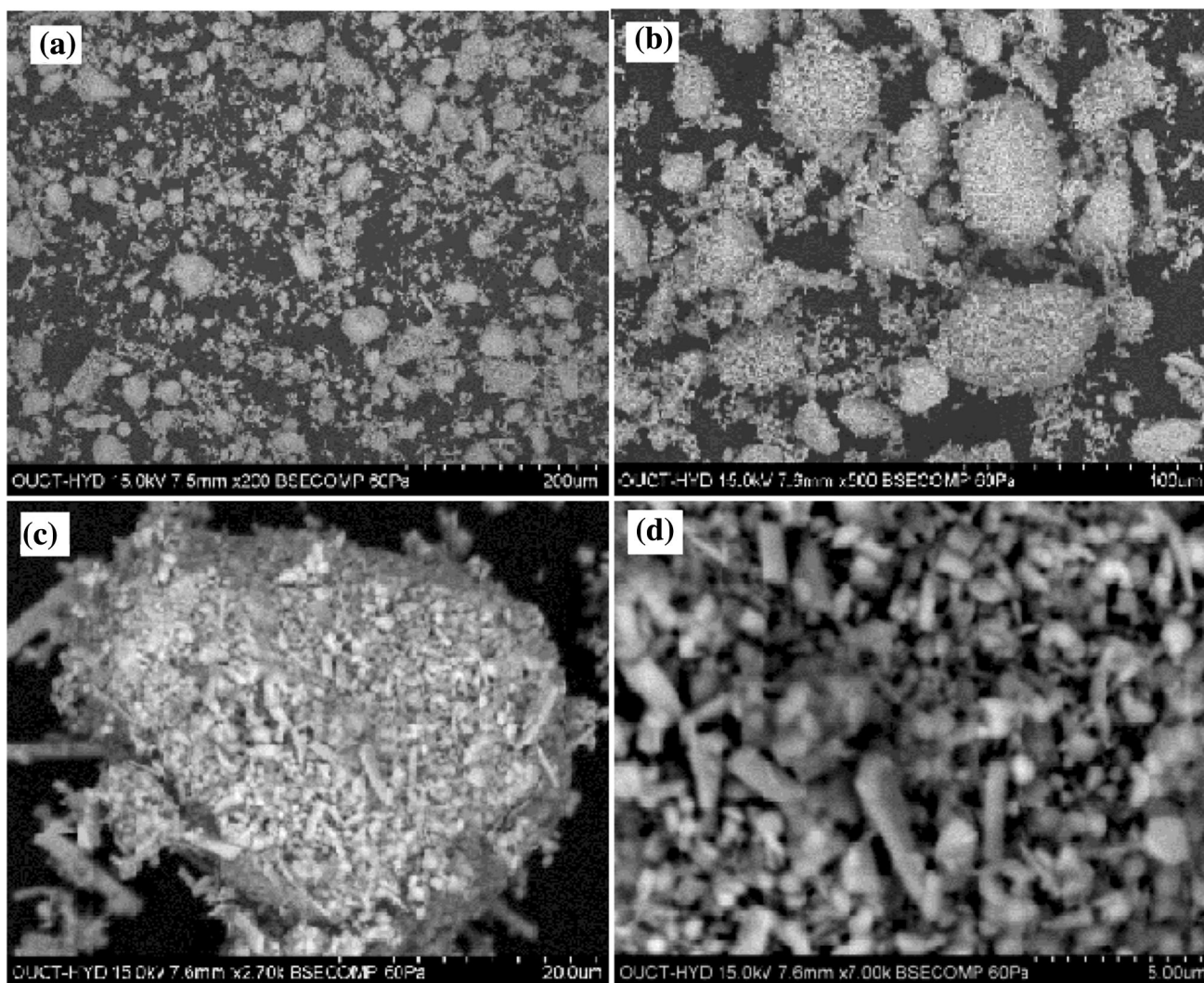


Fig. 3 SEM images of (a, b, c, d) 2.3:1 MoO₃-CuO metal oxide nanocomposite powders

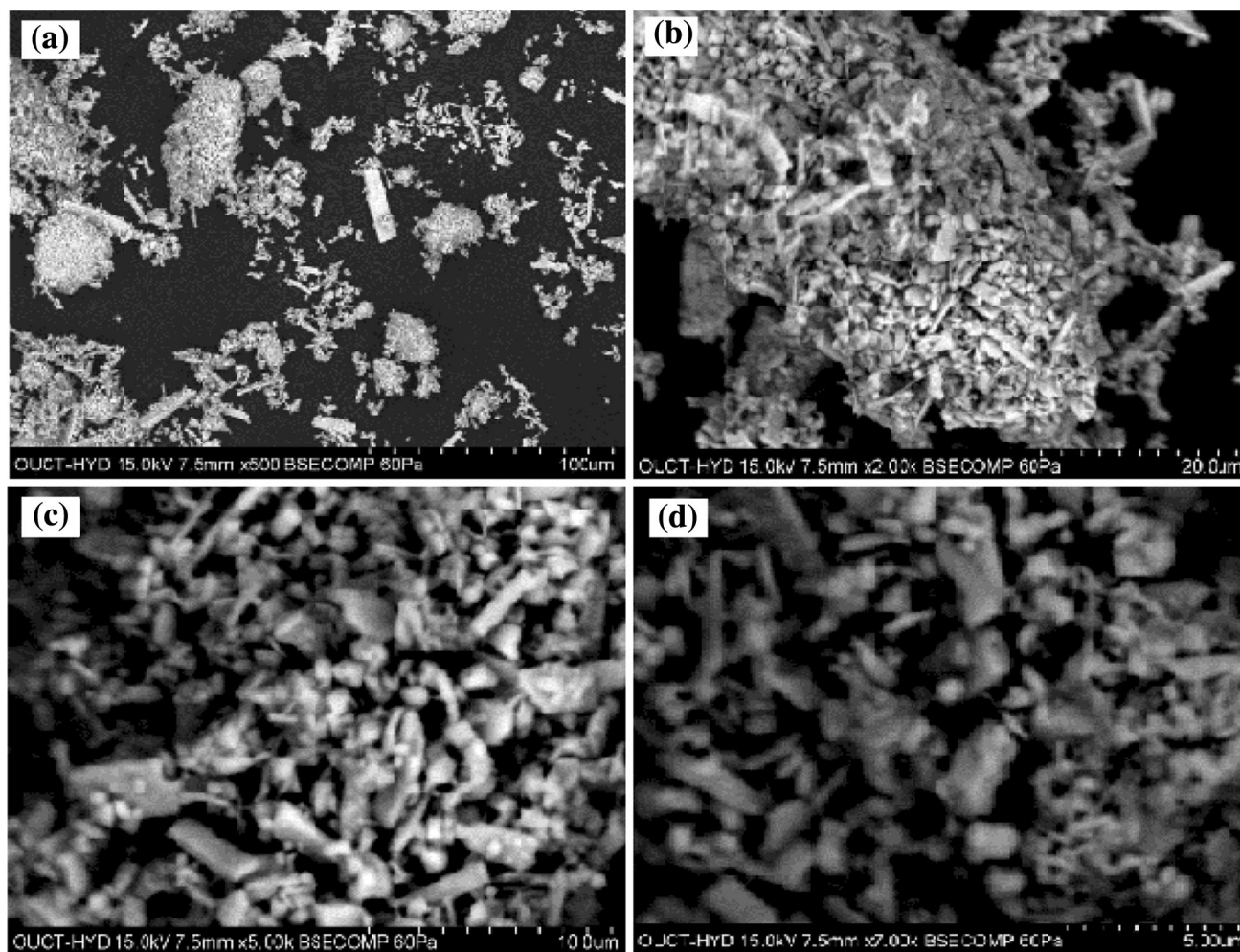


Fig. 4 SEM images of (a, b, c, d) 3.3:1 MoO₃-CuO metal oxide nanocomposite powders

mode of the Mo–OH bond and the bending mode of adsorbed water, respectively [45]. As the samples were calcinated at high temperatures, the presence of stretching and bending bonds is relatively low. The FT-IR bands of the two samples A and B are almost same and are as shown in Table 3, no shifting of peaks is observed.

Raman spectroscopy analysis

Crystalline quality can be effectively evaluated using the Raman spectroscopy. Figure 7 shows the Raman analysis bands corresponding to the characteristic phase of α -MoO₃ and β -CuO metal oxide nanocomposite. The vibrational mode assignments of MoO₃ and CuO are explained on the basis as described in the literature [46–48]. The number of physical properties of materials depends on the interactions between vibrational modes of molecules or lattices. According to the group theory, 24 Raman active modes are shown for (α -MoO₃) as $8A_g + 8B_{1g} + 4B_{2g} + 4B_{3g}$ [49].

The vibrations in the MoO₃ are due to the involvement of oxygen atoms, since the molybdenum atom is about six times heavier than oxygen atom. The vibrational modes occurring in the region of 1000–600 cm⁻¹ correspond to MoO₆ octahedral stretching modes and the modes between 400 and 200 cm⁻¹ and lower modes below 200 cm⁻¹ corresponds to MoO₆ octahedral bending vibrations and lattice modes [47–49]. From Fig. 7 two main absorption patterns are observed at 995, 819 cm⁻¹ which correspond to symmetric stretching vibrations of Mo=O and Mo–O–Mo. There is a slight shift in the peaks of sample B than sample A which is due to the more concentration of MoO₃. The Raman modes of MoO₃ in sample B show down shift of stretching vibrations from 819 to 813 cm⁻¹.

CuO belongs to the C_{2h}⁶ space group with two molecules per primitive cell. Out of nine optical modes only three ($A_g + 2B_g$) modes are Raman active and remaining six are IR active [48]. The interactions between the vibrational modes of molecules result in the number of physical



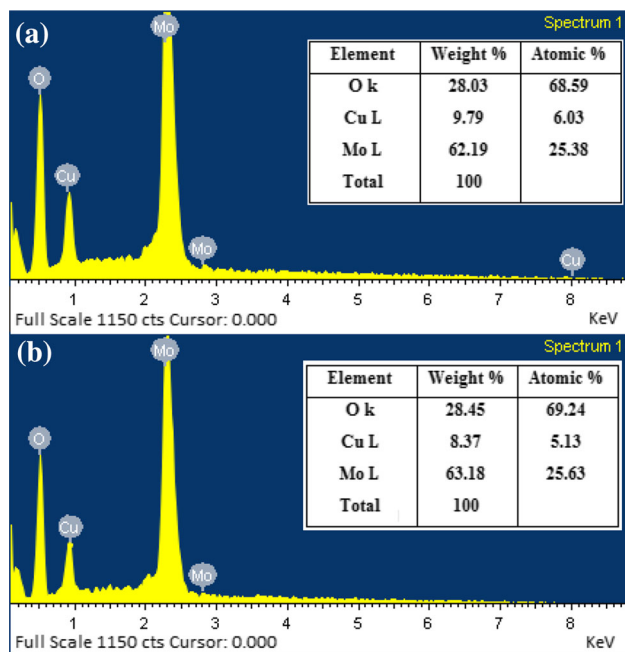


Fig. 5 EDS patterns of **a** 2.3:1 and **b** 3.3:1 MoO₃-CuO metal oxide nanocomposite powders

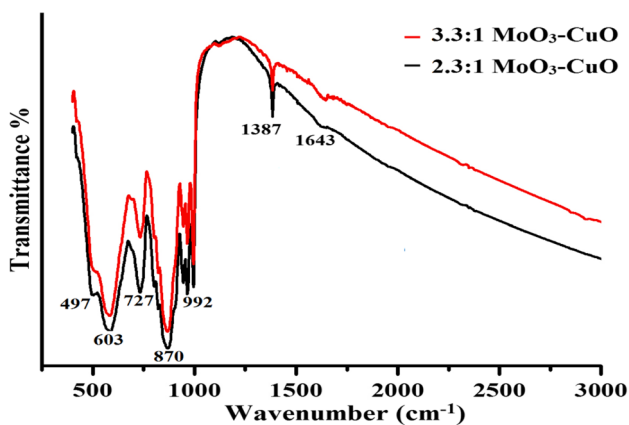


Fig. 6 FT-IR spectra of 2.3:1 and 3.3:1 MoO₃-CuO metal oxide nanocomposite powders

properties of materials. Only oxygen atoms move, with displacement in the b-direction for A_g and perpendicular to the b-axis for B_g Raman modes. The vibrational mode 298 cm⁻¹ corresponds to A_g and the bending vibrations 381 and 636 cm⁻¹ corresponds to the B_g modes [49].

TGA and DTA studies

To understand the thermal stability and relative weight loss of the material, Thermogravimetric Analysis (TGA) and Differential Thermal Analysis (DTA) play an important role. The analyses are performed under nitrogen atmosphere of 20 cm³ min⁻¹ at a ramp rate of 20 °C min⁻¹

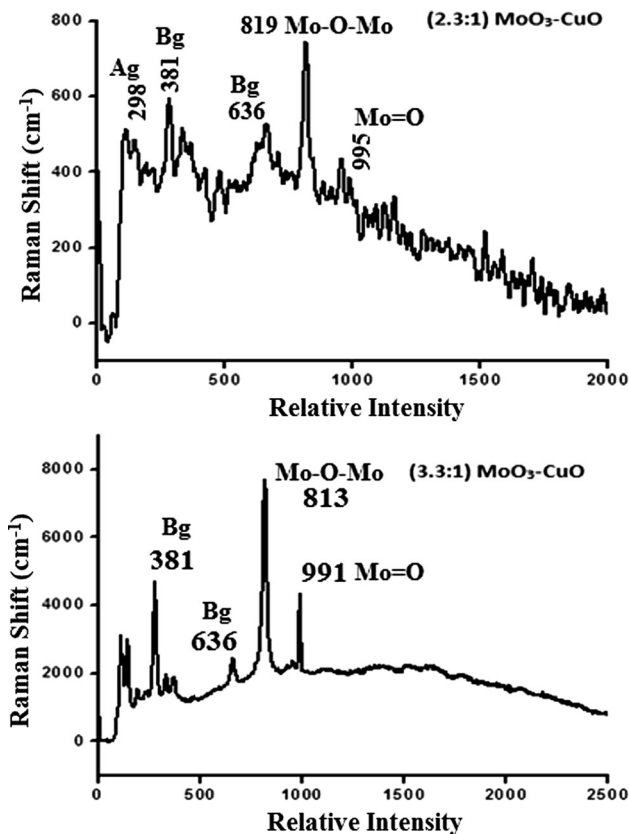


Fig. 7 Raman spectra of 2.3:1 and 3.3:1 MoO₃-CuO metal oxide nanocomposite powders

from 0 to 800 °C. The thermal analysis graphs are shown in the Fig. 8a, b. From Fig. 8a, b, it is noted that the ball-milled metal oxide nanocomposite powders are stable up to 709 °C as there is a negligible weight loss. The slight weight losses in the nanocomposites resulted in the graphs are mainly due to the evaporation of water molecules in the internal structure of the synthesised composite nanopowders. The corresponding band assignments are reported in Table 3.

Conclusions

Using a simple and inexpensive mechanical activation method, the synthesis of MoO₃-CuO metal oxide nanocomposite powders was prepared in weight ratios of 2.3:1 and 3.3:1. Powder XRD diffraction patterns of the prepared suggest the coexistence of dual phase structures, i.e. orthorhombic for MoO₃ and Monoclinic for CuO. The crystalline sizes were evaluated from the diffraction data through Debye–Scherrer’s formula which are in the order of nanometres and are counter verified by W–H method. Morphology obtained from SEM images confirms the irregular shaped particle sizes and EDS spectra confirms the presence

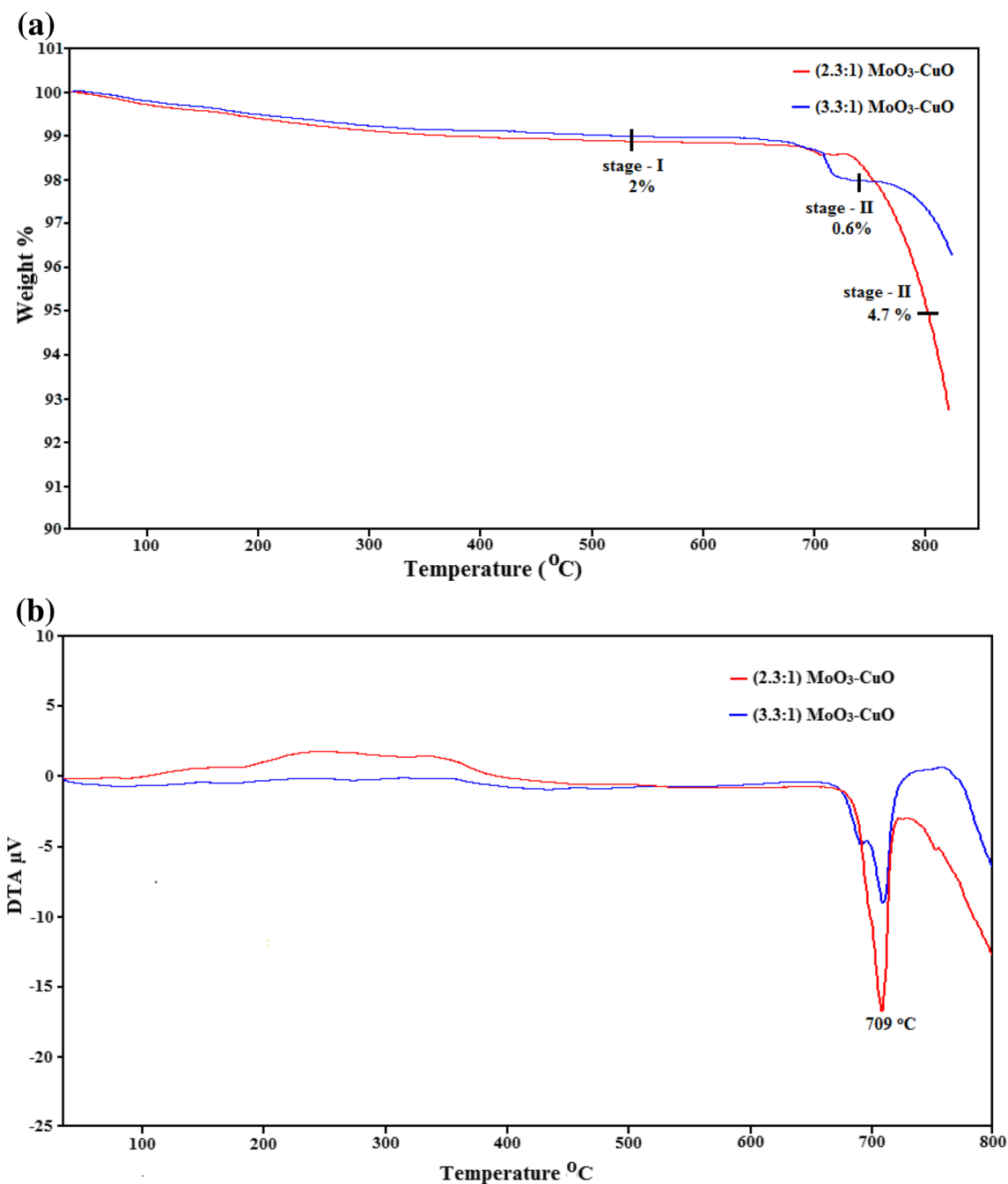


Fig. 8 **a** Thermogravimetric analysis and **b** Differential thermal analysis of (2.3:1 and 3.3:1) MoO₃-CuO metal oxide nanocomposite

of constituent elements of the prepared samples. The characteristic vibrational bands of MoO₃ and CuO are revealed through FT-IR spectrum. The qualitative information of the samples was obtained from Raman spectroscopy. TGA/DTA exhibited that the composite was stable up to 709 °C with negligible weight loss. Thus, the synthesised mixed metal oxide nanocomposite could be used as solid dry lubricant at high temperatures below 709 °C.

Highlights

- XRD reveals the metal oxide nanocomposite has coexistence of dual phase structures.
- Crystalline sizes calculated by Scherrer's equation are at nanosize levels which are confirmed by W-H analysis.



- TGA/DTA indicates that the MoO₃-CuO metal oxide nanocomposite powder withstand up to 709 °C with negligible weight loss.

Acknowledgments The authors Dola Sundeeep and S.Daniel Ephraim are thankful to the Director, Centralised Laboratory, Department of Physics, Acharya Nagarjuna University for providing the synthesis and spectroscopic measurement facilities such as XRD, FT-IR and TGA/DTA. Osmania University College of Technology (OUCT) for SEM and EDS. P.S.Subba Rao JNTUK for performing Raman Analysis and is thankful to AICTE, New Delhi, India for providing financial assistance through AICTE-GATE meritorious fellowship (1-1889699051) to carry out the research.

Compliance with ethical standards

Conflict of interest All authors declare that they do not have any financial or other conflict of interest.

Authors' contributions Sundeeep Dola (DS) has done the entire research with the help of co-authors. He has done the XRD Analysis and calculated the crystalline size, lattice parameters, dislocation densities and calculating the Williamson Hall plots. He has written the entire paper. Dr. A. Gopala Krishna (AGK) has analysed the vibrational bands from Raman spectra which confirm the phase structures revealed from the XRD. Dr. R. V. S. S. N Ravikumar (RR) has done the TG and DTA analysis and analysed the characteristic bands of FTIR graph. T. Vijaya Kumar (TV) has supplied the chemicals and done the SEM and EDS spectral analysis. S. Daniel Ephraim (DE) has done the synthesis part of the composite nanopowders through Ball-milling process in stoichiometric ratios. Y L Pavan (YP) has performed all mathematical calculation work. Hence I bring under to your kind notice that all the authors have equally shared the role in the research.

Open Access This article is distributed under the terms of the Creative Commons Attribution 4.0 International License (<http://creativecommons.org/licenses/by/4.0/>), which permits unrestricted use, distribution, and reproduction in any medium, provided you give appropriate credit to the original author(s) and the source, provide a link to the Creative Commons license, and indicate if changes were made.

References

- Walia, S., Balendhran, S., Nili, H., Zhuiykov, S., Rosengarten, G., Wang, Q.H., Bhaskaran, M., Sriram, S., Strano, M.S., Kalantar-Zadeh, K.: *J. Prog. Mater. Sci.* 1443–1489 (2013)
- Ordonez, S., Paredes, J.R., Diez, F.V.: *J. Appl. Cata. A General.* 174–180 (2008)
- Martinez, H.M., Torres, J., Rodriguez-Garcia, M.E., Carreno, L.D.L.: *Phy. B Condensed Matter* **407**, 3199 (2012)
- Hus, C.S., Chn, C.C., Huang, H.T., Peng, C.H., Hsu, W.C.: *J. Thin Solid Films* **516**, 4839 (2010)
- Battez, H., Rico, J.E.F., Arias, A.N., Rodrigues, J.L.V., Rodriguez, R.C., Fernandez, J.M.D. *J. Wear* **261**, 256–263 (2006)
- Xue, Q.J., Liu, W.M., Zhang, Z.J.: *J. Wear* **213**, 29–32 (1997)
- Hu, Z.S., Dong, J.X.: *J. Wear* **216**, 92–96 (1998)
- Sundeeep, D., Daniel Ephraim, S.: Use of nanotechnology in reduction of friction and wear. *IJIRAE*. **1**, 2349–2163 (2014)
- Yao, J.N., Hashimoro, K., Fujishima, A.: *Nature* **533**, 624–626 (1992)
- Hamelmn, F., Gesheva, K., Ivanova, T., Szekeres, A., Abroshev, M., Heinzmn, U.: *J. Optoelectron. Adv. Matter.* 393–399 (2005)
- Debecker, D.P., Stoyanova, M., Rodemerck, U., Gaigneux, E.M.: *J. Stud. Surf. Sci. Catal.* **175**, 581–585 (2010)
- Ganguly, A., George, R.: *J. Mater. Sci.* **30**, 183–185 (2007)
- Dong, W., Hung, H., Zhu, Y., Li, X., Wang, X., Li, C., Chen, B., Wang, G., Shi, Z.: *J. Nanotechnol* **23**, 425602 (2012)
- Wang, J.F., Rose, K.C., Lieber, C.M.: *J. Phys. Chem. B* **103**, 8405–8409 (1999)
- Song, J., Li, Y., Zhu, X., Zhao, S., Hu, Y., Hu, G.: *Mater. Lett.* **95**, 190–192 (2013)
- Nirupama, V., Uthanna, S.: *J. Mater. Sci.: Mater. Electron.* **21**, 45–52 (2010)
- Badica, P.: *J. Cryst. Growth Des.* **7**, 794–801 (2007)
- Chernova, N.A., Roppolo, M., Dillon, A.C., Whittingham, M.S.: *J. Mater. Chem.* **19**, 2526–2552 (2009)
- Marabelli, F., Parravicini, G.B., Salghetti-Drioli, F.: *J. Phys Rev B* **52**, 1433–1436 (1995)
- Hernandez Battez, A., Viesca, J.L., Gonzalez, R., Balnco, D., Asedegbega, E., Osorio, A.: *Wear.* 325–328 (2010)
- Mark A. Kedzierski.: *Int. J. Refrig.* 1997–2002 (2012)
- Quinn, T.F., Winer, W.O.: *J. Wear.* **102**, 67–68 (1985)
- Peterson, M.B., Calabrese, S.J., Li, S.Z., Jiang, X.X.: *J. Mater. Sci. Tech.* 313–318 (1994)
- Sliney, H.E.: Rare Earth fluorides and oxides; an exploratory study of their use as solid lubricants at temperatures to 1800 °F. NASA TN D-5301 (1969)
- Peterson, M.B., Calabrese S.B., Stupp, B.: Lubrication with naturally occurring double oxide films, Office of Naval Research, Final Report, Contract No: N00014-82-C-0247 (1982)
- Wahl, K.J., Seitzman, L.E., Bolster, R.N., Singer, I.L., Peterson, M.B.: Ion beam deposition Cu-Mo coatings as high temperature solid lubricants [J]. *Surf. Coat. Technol* **9**, 245–251 (1997)
- Murty, B.S., Ranganathan, S.: *Int. Mater. Rev.* **43**, 101 (1998)
- Wang, L, Fu, X., Han, Y., Chang, E., Wu, H., Wang, H., Li, K., Qi, X.: *J. Nanomater.* 321459 (2013)
- Chang, Tongqin, Li, Zijiong, Yun, Goaqian, Jia, Yong, Yang, Hongjun: *Nano-micro Lett* **5**, 163–168 (2013)
- Zabinski, J.S., Day, A.E., Donley, M.S., Dellorcorte, C., Mc, N.T.: Devitt. *J. Mater. Sci.* **29**, 5875–5879 (1994)
- Naussau, K., Shiever, J.W.: *J. Am. Ceramic Soc* **52**, 36–40 (1969)
- Machej, T., Ziolkowski, J.: *J. Mater. Chem.* 113–121 (1979)
- Murugadoss, G.: *J. Particuol* **10**, 722–728 (2012)
- Cullity, B.D., Stock, S.R.: *Elements of X-ray Diffraction*, 3rd edn. India: Prentice Hall Publication (2001)
- Patterson, A.J.: *Phys. Rev.* **56**(10), 978–982 (1939)
- Thirumala Rao, G., Babu, B., Joyce Stella, R., Pushpa Manjari, V., Ravikumar, R.V.S.S.N.: *J. Spectrochim. Acta Part A Mol. Biomol. Spectrosc.* 139 (2015)
- Joyce Stella, R., Thirumala Rao, G., Pushpa Manjari, V., Ch. Rama Krishna, B., Babu, J.: *Alloys and Compounds.* **628**, 39–45 (2015)
- VD Mote, Purushotham and BN Dole.: *J. Theor. Appl. Phy.* **6**:6 (2012)
- Suryanarayana, C., Norton, M.G.: *X-ray Diffraction: a Particle Approach.* Plenum Press Publishing, New York (1998)
- Zak, A.K., AbdMajid, W.H., Abrishami, M.E., Yousefi, R.: *Solid State Sci.* **13**, 251 (2011)
- Natarajan, G., Daniels, S., Cameron, D.C., Reilly, L.O., Mitra, A., McNally, P.J., Lucas, O.F., Rajendra Kumar, R.T., Reid, I., Bradley, A.L.: *J. Appl. Phys.* **100**, 033520 (2006)
- Kliche, K., Popovic, Z.V.: *J. Phys Rev B* **190**(42), 10060–10066 (1990)
- Segun, L., Figlaz, M., Cavagnat, R., Lassegues, J.C.: *Spectr. Acta A* **51**, 1323 (1995)



44. Harb, F., Gerand, B., Nowogrocki, G., Figlitz, M.: *J. Sol. State Ionics* **32–33**, 84 (1989)
45. Chithambararaj, A., Chandra Bose. A.: *Beilstein J. Nanotechnol.* **2**, 585–592 (2011)
46. Yao, D.D., Ou, J.Z., Latham, K., Zhuiykov, S., O'Mullane, A.P., Kalantar-zadeh, K.: *Cryst. Growth Des.* **12**, 1865 (2012)
47. Atuchin, V.V., Gavrilova, T.A., Grigorieva, T.I., Kuratieva, N.V., Okotrub, K.A., Pervukhina, N.V., Surovtsev, N.V.: *J. Cryst. Growth* **318**, 987 (2011)
48. Xu, J.F., Ji, W., Shen, Z.X., Li, W.S., Tang, S.H., Ye, X.R., Jia, D.Z., Xin, X.Q.: *J. Raman Spectrosc.* **30**, 413–415 (1999)
49. Seguin, L., Figlitz, M., Cavagnat, R., Lassgues, J.C., Spect, J.: *Acta Part A* **51**, 1323–1344 (1995)

Dola Sundeep Received his graduation in Electronics and Communication Engineering in 2013 and Master's degree in Nanotechnology in 2015 from Jawaharlal Nehru Technological University Kakinada, India. He is presently working as Research Scholar in JNT University Kakinada. His area of research is on High Temperature Solid Lubricant Nanocomposites, Nanoelectronics and Nanosensors. He holds an associate membership in Institute of Engineers India (IEI).

A. Gopala Krishna is working as Professor of Mechanical Engineering and Head of School of Nanotechnology in Jawaharlal Nehru Technological University Kakinada. He obtained his graduation in Mechanical Engineering in 1994 and Master's degree in Mechanical Engineering from S.V University, Tirupathi, India in 1996. He received his doctorate degree (PhD) in Mechanical Engineering from JNT University, Kakinada, India in 2006. He is a life member of ISTE and Institution of Engineers (IEI), India.

R. V. S. S. N. Ravikumar is working as Assistant Professor of Physics in Acharya Nagarjuna University, Guntur, India. He received his graduation in Science (1988) from Andhra University and M. Sc (1992), M.Phil (1996) and Phd (1997) in physics from S.V University, Tirupathi, India. He worked as Post-Doctoral Fellow in Advanced Materials Sciences and Engineering in Yamaguchi University, Ube, Japan in 2003 and in chemistry in Kyoto University, Kyoto, Japan in 2005. He also worked as a CSIR pool scientist in Pondicherry University, India. He published around 150 papers in international journals and 230 papers in national and international conferences.

T. Vijaya Kumar is working as Assistant Professor and Research Scholar in K L University, Guntur, India. He received his graduation in Mechanical Engineering from Acharya Nagarjuna University in 2000 and Master's degree in Material Science and Technology from National Institute of Technology (NIT) Calicut, India. He is working on Nanocomposites for Solid Lubrication.

S. Daniel Ephraim received his graduation in Mechanical Engineering in 2011 and Master's degree in Machine Design in 2015 from Jawaharlal Nehru Technological University Kakinada, India. He had worked as Assistant Professor for 3 years and now started working on Nanocomposites for Tribology.

Y. L. Pavan received his graduation (2013) and Master's (2014) degree in Mechanical Engineering from K L University, Guntur, India. He is working as Mechanical Engineering in FMC Technologies, India.

